E.2 SCIENTIFIC GOALS & OBJECTIVES

E.2.1 NEED FOR SIMULTANEOUS, HIGH RESOLUTION IMAGING AND SPECTROSCOPY

No spectroscopic observations are currently possible at the spatial and temporal scales characteristic of the solar chromosphere and TR. These spatial and temporal scales, which are summarized in the next few paragraphs, are known almost exclusively from imaging. To learn the underlying physics of these phenomena, we need spectroscopic measurements with simultaneous, perfectly co-aligned, high-resolution context imaging; such observations enable the measurement of 3D flows, temperature changes, non-thermal effects, and wave properties. These observations are exactly what IRIS is designed to provide (for detailed instrument requirements, see §D.3).

Ground-based Hα observations at La Palma reveal fibrils with widths for the smallest structures down to the resolution limit, close to 120 km (0.16 arcsec)[7]. Recent Hinode/SOT Ca II H limb movies reveal thin spicular structures with widths as small as 0.2 arcsec, which persist for intervals of only 10-100s before they fade away[2]. Transverse motions in the field appear to occur with amplitudes of up to 20 km/s, with displacements of ~1-3 arcseconds in 3-5 min, traced fleetingly as the spicules show up and fade away[1].

Much of this structuring in chromosphere and TR is an inevitable consequence of the underlying photospheric evolution of the field: magnetic flux emerges constantly, and flux tubes caught in granular downflows fragment or cluster while spiraling around others in turbulent vortices as they are buffeted by a complex wave field. As they are moved about, they interact among themselves and with emerging flux in strong-field ephemeral regions and in the vast pool of small-scale internetwork field with a range of strengths[8].

The 0.33-04 arcsec resolution of IRIS will provide a major leap forward compared to current capabilities as shown by the analysis of high-resolution observations with Hinode's SOT and the best ground-based telescopes. These observations show that the chromosphere is dominated by features with structuring perpendicular to the magnetic field below the 2" resolution achievable with current space-based spectrographs (similar for both SOHO/SUMER and Hinode/EIS). Hinode/SOT limb observations in the Ca II H filter reveal a histogram of feature cross sections that peaks at about 350 km (Fig. CSR-A, bottom), and

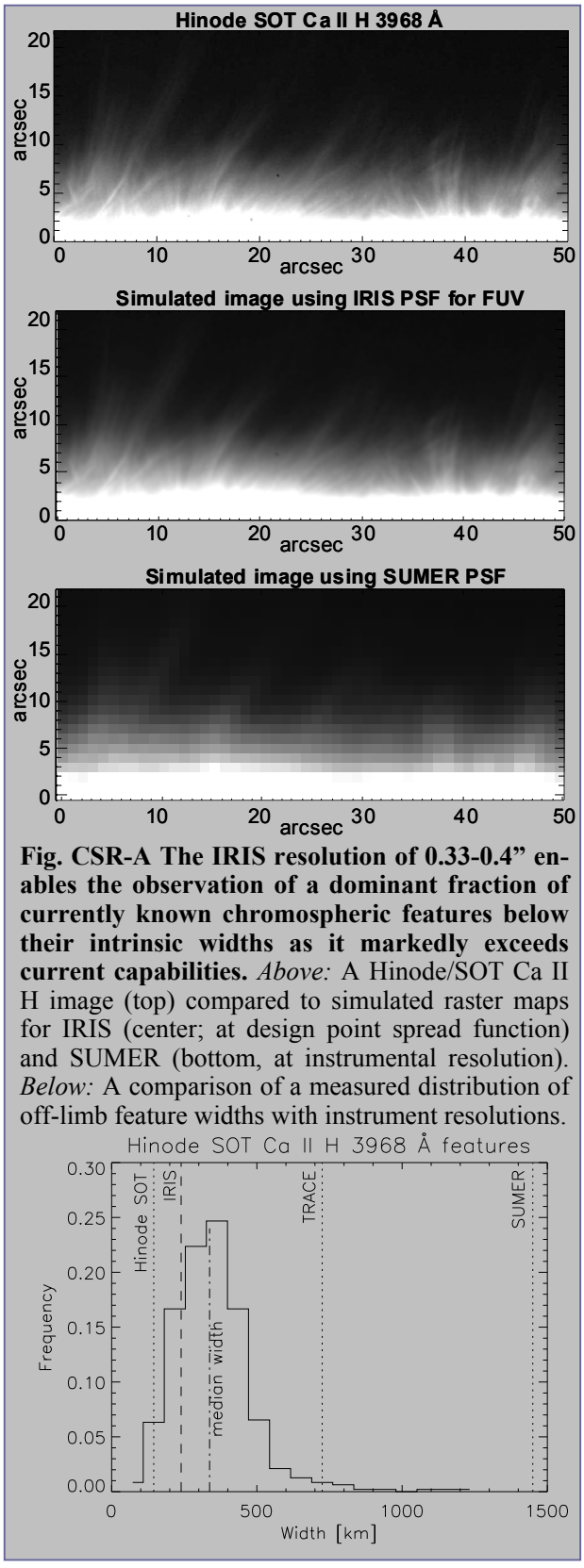

Fig. CSR-A The IRIS resolution of 0.33-0.4" enables the observation of a dominant fraction of currently known chromospheric features below their intrinsic widths as it markedly exceeds current capabilities. *Above:* A Hinode/SOT Ca II H image (top) compared to simulated raster maps for IRIS (center; at design point spread function) and SUMER (bottom, at instrumental resolution). *Below:* A comparison of a measured distribution of off-limb feature widths with instrument resolutions.

has many structures above the 0.33-0.4 arcsec design resolution of IRIS. Consequently, IRIS will be the first orbiting UV spectrograph to observe the chromosphere and TR simultaneously with the potential of resolving many of the features that we know to exist from chromospheric imaging systems[2, 77] while drastically reducing the number of such features in any line of sight.

The dramatic improvement of IRIS relative to earlier UV spectrographs is illustrated in Fig. CSR-A (top), which compares a Ca II H image by Hinode's SOT to the future IRIS resolution and the existing SOHO/SUMER (and Hinode/EIS) resolution – these images were computed by convolving the instrument point spread functions (PSFs) with a deconvolved SOT image. We also note that the coherence scale of near-photospheric waves exceeds the IRIS resolution: even at the 1-arcsec TRACE resolution the wave power was measured to be within 20% of that now seen with Hinode's SOT[24]. Thus, the IRIS PSF will enable very significant advances relative to current UV spectroscopic capabilities, resolving most of the currently known features and the bulk of the available acoustic wave power in near-photospheric layers.

Although we think we understand the basic reasons for the chromosphere's highly dynamic and structured state, we really do not understand the relative roles of the candidate processes in the chromospheric and TR energy balance. The fundamental problem of how non-thermal energy from below the solar surface is transported and released to shape the dynamic solar atmosphere involves many detailed questions that include:

- How much of the energy flux associated with flux emergence in the mixed-polarity "magnetic carpet" makes it into the corona or wind?
- In what forms does most energy travel upward?
- How important are braiding[11,12,13] and torsional motions (now for the first time directly observed by Hinode's SOT) by footpoint displacements to the solar atmosphere?
- Where do the motion-induced currents run and where are they most strongly dissipated?

A variety of MHD waves[14] complements the overall upward flow of energy (Fig. E-2) that powers the corona and solar wind, but their relative contributions remain uncertain[15]. It is even less clear which wave types play a role where. Transverse waves, for example, travel fairly easily through the stratified atmosphere[1] with its complex magnetic field with alternating near-horizontal weak canopies and near-vertical stalks of strong field, but in doing so they are subject to reflections and conversion into other modes that include longitudinal and mixed-mode waves. Moreover, coronal intensity oscillations observed by TRACE[16,17] revealed that sound waves can travel with increased ease into the corona wherever inclined field effectively reduces gravity, thereby lowering the acoustic cutoff frequency[18]. The combination of imaging and spectroscopy at high resolution will enable the IRIS team to measure the power in various types of MHD

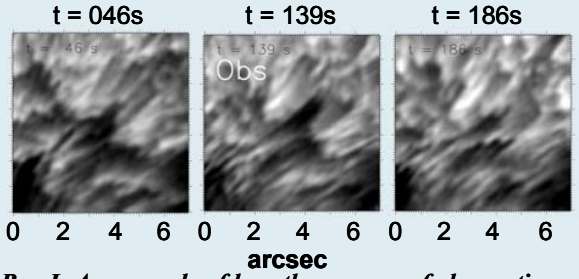

Box I: An example of how the synergy of observations and modeling advances understanding:

Observations often reveal the unexpected. They are also necessary to validate choices made by numerical modelers on how physical processes are approximated in their codes. Numerical models, on the other hand, can show phenomena in a way that observations cannot. The IRIS investigation considers both aspects to be crucial to success, and includes them as equal partners.

For example, spicules (as seen in, for example, Hα, above) long defied understanding[9]. Then, space-time diagrams of remarkable quality were made from high-quality, high-resolution observations (top panel below). These revealed ubiquitous parabolic trajectories. Upon realizing that these form when shock waves pass through the chromosphere, 3D models shortly thereafter were found to show very similar phenomena (bottom panels below), unambiguously showing that "Dynamic Fibrils Are Driven by Magnetoacoustic Shocks"[10]. The finer "type-II spicules" in Ca II H Hinode observations remain mysterious[1], even as they serve as wave diagnostics – see Box II

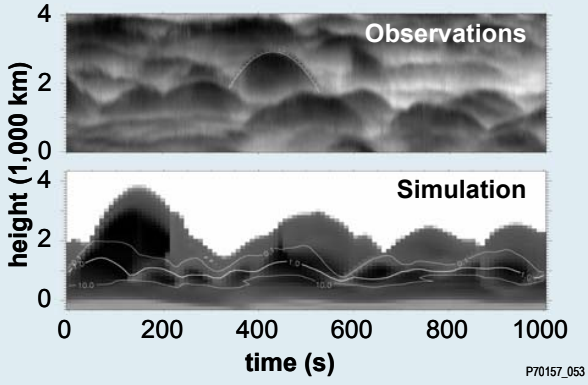

waves, see where these waves are dissipated, converted, or reflected, and establish how MHD waves contribute to the energetics of the solar atmosphere (see §E.2.2).

In the high chromosphere and TR, energy coming down from the corona affects the stratification and causes mass exchange between chromosphere and corona. Whether conducted as thermal energy or propagating as energetic particles originating in reconnection events, this energy causes chromospheric material to heat up and flow upward into the corona, both in quiescense and in flares[19,20]. Here, too, small scales are involved: reconnection likely involves a turbulent cascade to scales well below observable ones[13].

Moreover, the spatio-temporal relationship between lower-chromospheric and coronal heating remains unclear: it is puzzling that there is no significant correlation between the TR EUV emission (as a tracer of coronal heating) and the chromospheric Ca II emission at the TRACE resolution of 1.25 arcsec and ~12s[21]. Perhaps this signifies that although coronal and chromospheric heating are both related to the magnetic field, they do not occur simultaneously or similarly in these two regions. At the very least, it means that we cannot trace the connections of field, energy, and matter from photosphere to corona from single snapshots, because even if these cover the wide range of temperatures required, the temporal evolution of the moving plasma needs to be observed as well. This, too, requires high resolution, combined with a large range of temperatures: IRIS will provide access to the evolving chromosphere, TR, and corona with high cadence and resolution to enable us to use propagating perturbations and plasma flows to probe the structure of the solar atmosphere, with modeling and context observations by, e.g., SDO and Hinode to help interpret the data. In order to figure out which non-thermal processes dominate, IRIS needs to get close to resolving the thermal line widths in these regions.

Both observations and models show that subarcsecond resolution and cadences of no more than tens of seconds are required. We must also measure line-of-sight velocities to determine the 3D flow vectors, and the thermal evolution of the plasma to track plasma as it changes temperature.

E.2.2 RESEARCH THEMES & METHODS

IRIS will resolve in space, time, and wavelength the dynamic geometry from the chromosphere to the low-temperature corona to shed much-needed light on the physics of this magnetic interface region: we will be able to follow plasma up- and down-flows at high resolution, measure the wave and heat fluxes associated with these flows, measure transverse plasma displacements and model the associated changes in the field, and have access to any non-thermal processes that reveal themselves only as line broadening even at 1/3 arcsecond resolution. To characterize the science investigation, we identify three research themes that together define the scientific requirements (see Table FO1-1; discussed in §E.3):

a) Which types of non-thermal energy dominate in the chromosphere and beyond?

We still do not know which modes of non-thermal energy power the chromosphere, TR, corona, and solar wind (see Fig. E-1). We know that waves, electrical currents, and magnetic reconnection all may release substantial energy, and that non-thermal particles, resistive dissipation, and wave damping occur. Yet, it remains unclear how much each of these contributes, how that depends on local conditions, and how the conversion of non-thermal to thermal energy happens in detail.

Waves: The role of virtually pure acoustic power in the heating of the chromosphere and its potential role in the corona remains a puzzle: some report too little power[22,23,24], while others argue there should be enough[25,26,27]. TRACE, Hinode, and ground-based Hα observations recently revealed that the parabolic trajectories of many spicules are caused by magneto-acoustic shocks (Box I). IRIS provides the spectroscopic data to follow compressible magneto-acoustic waves from the photosphere (in neutral lines in the far-UV) into the corona (using, e.g., Fe XII) by measuring phase delays, amplitudes, and line profiles as a function of temperature in different magnetic geometries (Fig. E-3). Most of the power in these modes lies in the range of the 5-min *p*-mode spectrum and the 10-15 min time scale of granular evolution, but waves have been measured for periods as short as ~25 s[23] although the power in these waves is over 4 orders of magnitude less than at the peak of the 5-min range. IRIS' temporal cadence of seconds for individual spectra enables us to measure a wide range of wave periods (Fig. E-3), even when spectral maps are constructed by rastering small areas.

Various types of (mostly transverse) MHD waves are likely more efficient at traveling into the corona and solar wind[29,30] than mostly compressible waves. These will be studied by combining spectroscopy with imaging. Numerical experiments and observations both show the chromosphere to be continually undulating, threaded

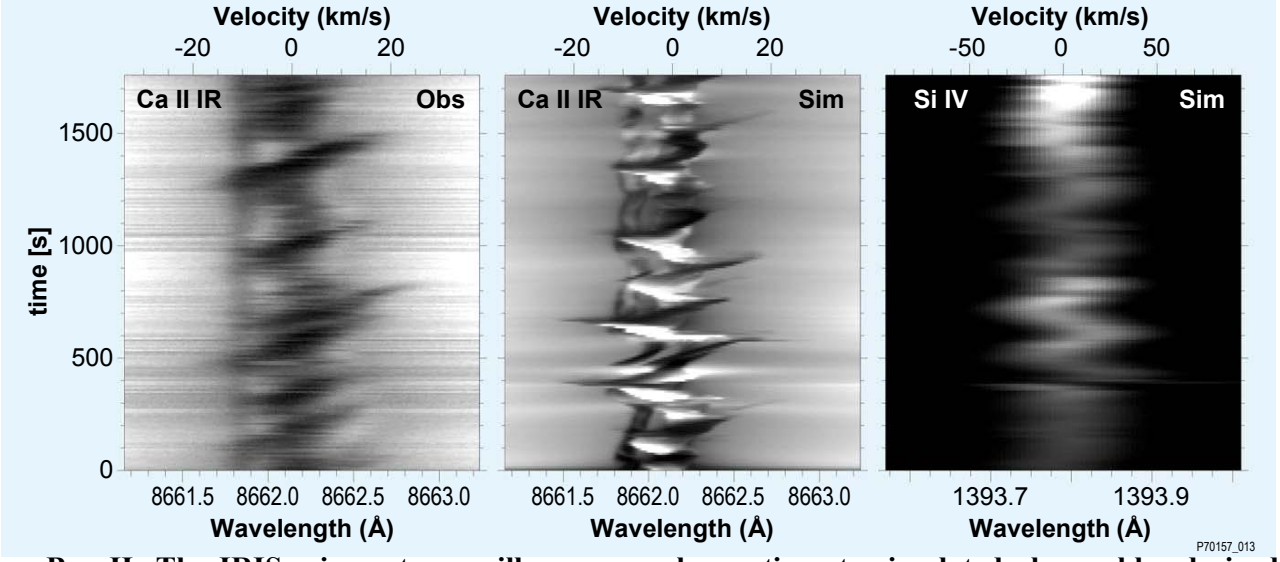

Box II: The IRIS science team will compare observations to simulated observables derived from highly realistic numerical experiments to guide models to higher fidelity and scientists to a deeper understanding. *Radiative MHD models already allow the computation of line profiles in 2D, both for optically thin and for optically thick lines formed in the chromosphere and TR, and early 3D models are being tested for small volumes; model capabilities will continue to advance.*

Example: The figure above reflects the current state of the art for 2D results for optically thick and thin radiative MHD. It compares an observed wavelength (λ)−time diagram for the Ca II IR triplet (left) with 2D radiative-MHD simulations for the optically thick Ca II IR signal (center) and for an approximated optically-thin Si IV signal (right) such as IRIS can observe. Supported by such modeling, IRIS will enable the tracking of MHD waves through the chromosphere (observed in both Mg II emission and in UV emission lines) into higher-temperature domains, up to the low corona. The figure below shows a preview of 3D MHD modeling for optically thin radiation: it shows simulated emission of a network region as observable with IRIS spectral raster maps; intensity (left) and Doppler shift (right) are shown as expected at the solar limb (upper) and at disk center (lower). Further advances to be made on the modeling front are a mix of technical issues (parallelization and mesh refinement) and physical processes (including small-scale reconnection, time-dependent ionization[28], high-energy particle populations, and non-MHD effects such as multi-fluid descriptions and anomalous resistivity. Detailed comparisons of IRIS observations with the anticipated results from such advanced models, enables us to understand the relative importance of plasma-physical processes in chromosphere and TR.

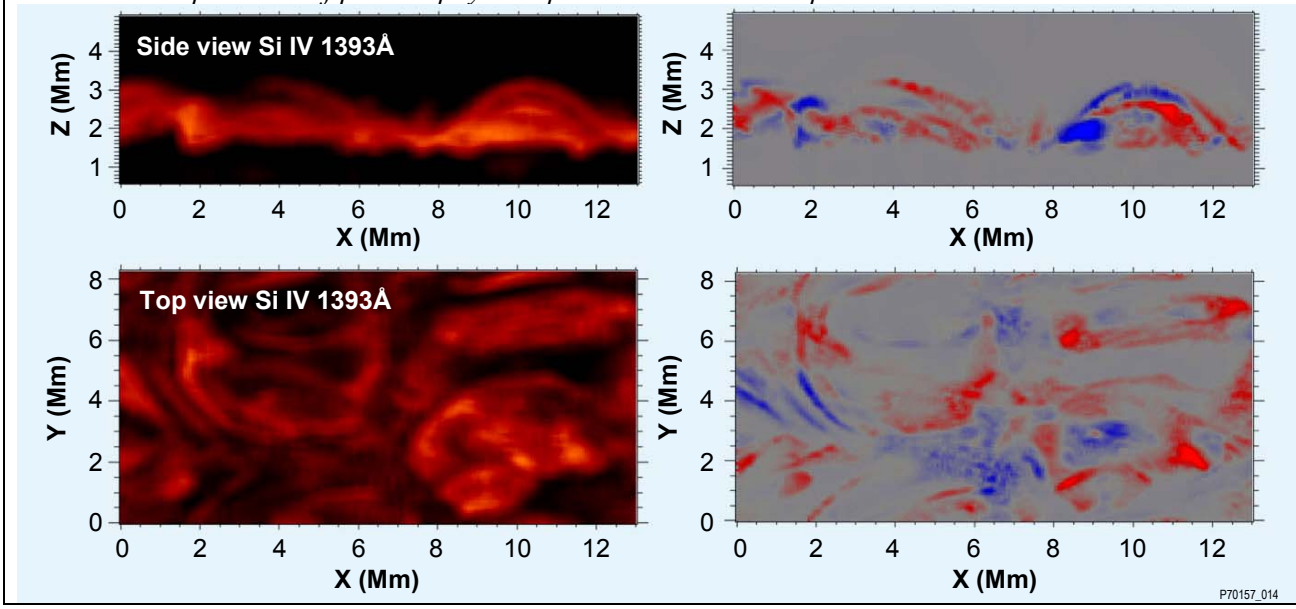

by a swaying magnetic field (Fig. E-4). Hinode recently observed these motions in the highest layers of the chromosphere in Ca II H movies[1]. Much of the non-thermal line widths seen with spectrographs such as SOHO's SUMER may well be caused by these waves[31], which are prime candidates for powering the solar wind. In the closed corona, they may be less important energetically, but there they serve valuable diagnostic purposes in coronal seismology[32].

With IRIS we aim to measure the energy fluxes in both longitudinal and transverse waves traversing the chromosphere and TR to understand their propagation, reflection, and damping properties better than we do at present. Radiative MHD modeling will be guided by IRIS's observations and will in turn guide the interpretation of the measurements (Fig. E-3). We will do this in complementary ways (see also Box II). For example, Doppler shifts and transverse motions (measured using the spectrograph's slit-jaw images or maps made by stepping the spectrograph slit) will provide statistical information on the wave fields. Doppler shifts will be measured to 0.5 km/s, which is well below the local sound and Alfven speeds in the chromosphere (typically 5 to 20 km/s); line profiles constrain line-of-sight superposition of structures. Different viewing angles from disk center to limb will be used to statistically study anisotropies, both to differentiate transverse from longitudinal components and to constrain sub-resolution amplitudes through anisotropic line broadening.

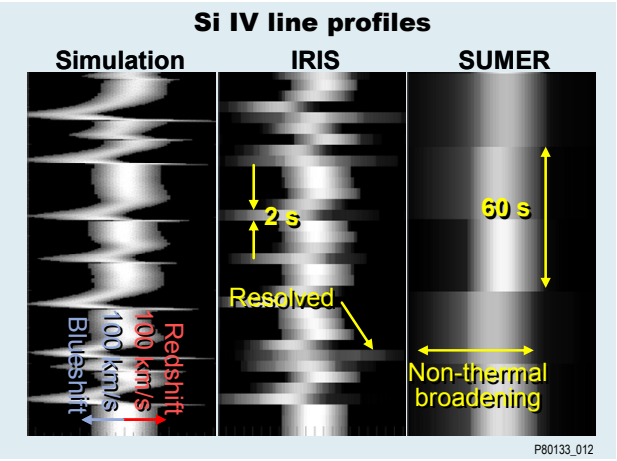

Fig. E-3 IRIS will be able to observe high-frequency waves down to 0.2 Hz. *IRIS data (center) will provide constraints to nanoflare model results[36] (left), which current SUMER data cannot do (right).*

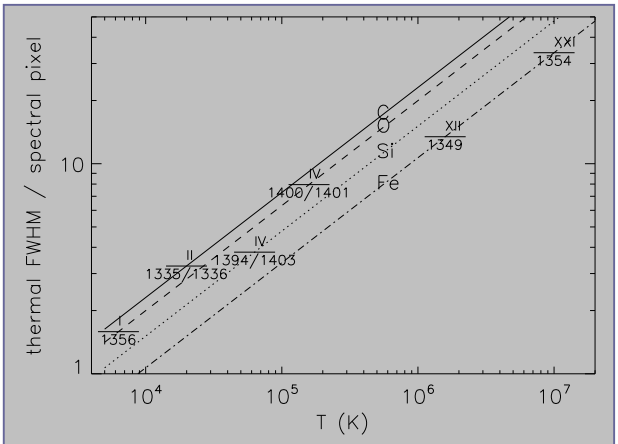

Fig. CSR-B The wavelength windows selected for the IRIS UV spectrograph contain relatively strong spectral lines that span the thermal range from below 10^4K to 10^7K. The dispersion allows centroiding to well below the local sound speeds.

The panel above shows a selection of the strongest lines (not showing the optically-thick Mg II lines), and compares their thermal widths with the IRIS spectrograph pixel size.

The dispersion for IRIS spreads thermally broadened spectral lines over multiple CCD pixels (with non-thermal broadening adding to that). The Doppler shifts in line center position can thereby be determined to a fraction of a pixel, or better than ~0.5 km/s, well below the local sound speed. The lower panel in this box summarizes a simple experiment to illustrate this: 1000 realizations are made for 1.2s exposures of quiet Sun in Si IV 1394Å plus continuum, including realistic IRIS throughput, photon noise, and detector read noise. Fitting gaussians and a background level to these simulated profiles yields a distribution with a standard deviation of 0.16 pixels, or 0.42 km/s, below the science requirement of ~0.5 km/s.

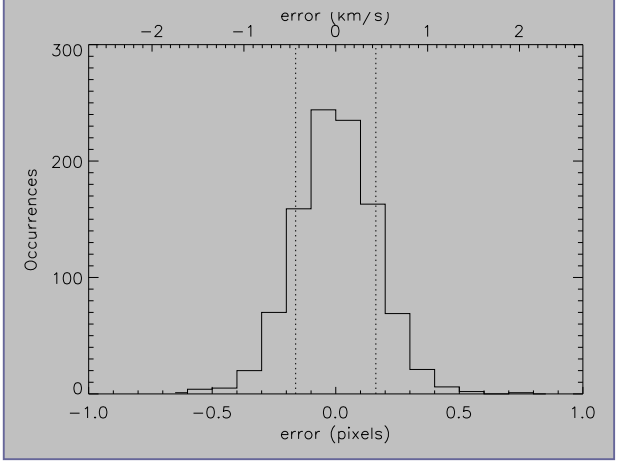

Detailed measurements of the propagation of waves relative to the magnetic field can be made by combining IRIS observations with vector-magnetic field extrapolations (based on, among others, Hinode's SOT-SP, using nonlinear force free [NLFFF][33,34] or magnetostatic models[35]) or more directly with the directions of chromospheric fibrils seen in IRIS Mg II k slit-jaw images.

High-cadence observations combined with modeling allow us to quantify reflection, transmission, and absorption of the waves. Imaging with a ~10s cadence, and repeating spectrograph maps of areas up to 3 arcsec wide with that same cadence, enables the study of waves with periods down to 20 s. At a fixed position, spectra can be obtained to study waves with periods down to 2 s.

The ultimate goal is forward modeling of radiative MHD, guided by IRIS's observations and coordinated vector-magnetic field observations. As future-generation models are developed, these will provide sufficient realism in field-plasma coupling, radiative transfer, energy deposition, and wave properties for a direct comparison.

Currents: Establishing the energy associated with resistive dissipation of electrical currents within the chromosphere is challenging. We expect these currents to be intense in compact fibrils or sheets. Any dissipation within the chromosphere is expected to be associated with rapid temperature increases. IRIS will enable the spectroscopic tracing of changes in the thermal structure even in very thin strands. Such strands are seen with Hinode's SOT in Ca II H for only some tens of seconds[1,2], possibly because changes in temperature cause them to fade from the passband. The broad thermal coverage of IRIS spectra and images from 5,000 to over a hundred thousand Kelvin will allow us to follow such an evolution.

The evolution of the thermal structure within the chromosphere will provide information on how much electromagnetic energy is transformed locally into heat and how much energy propagates downward from the corona as thermal energy or energetic particles[37,13] in events ranging from microflares to X-class flares. We expect both to occur, of course, but do not know their relative roles under a variety of conditions.

Local heating and heating from above: Observations at high resolution should enable us to solve the problem that we still cannot present a comprehensive model of TR and corona that satisfies observational constraints: the corona appears to be dynamically evolving much of the time, leading to strands of plasma at different thermal and density stratifications evolving in close proximity, but so far neither stationary nor dynamic models match the TR emission unless a considerable expansion of the field with height is included; unfortunately, such strong expansions are not supported by direct observations[38,39]. IRIS's high resolution for a range of temperatures will help us address this mystery: we will see the field geometry reflected in the images, while spectroscopic data will help us study the role of dynamics in the high chromosphere and TR[37].

b) How does the chromosphere regulate mass and energy supply to corona and heliosphere?

The heating of the solar corona and the acceleration of the solar wind remain mysteries[40,41]. IRIS aims to contribute to their resolution by

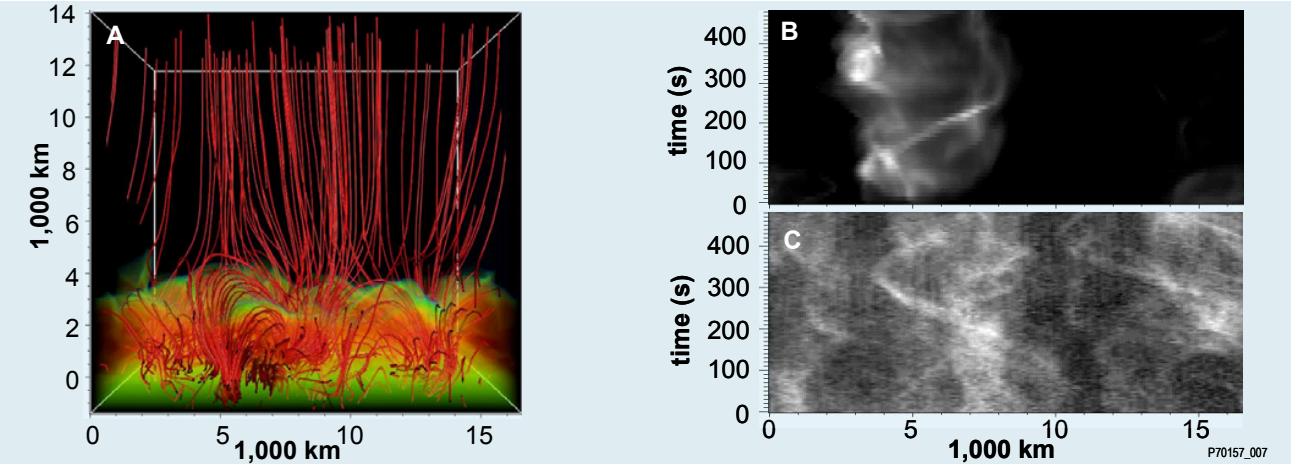

Fig. E-4 Numerical experiments approach reality as in this simulation (A) of the chromosphere over quiet-Sun magnetoconvection[1]. The swaying of the field, visualized in a time-space diagram for simulated Ca II H emission (B) is similar to that in Hinode's SOT limb observations (C) [see Box II].

showing us in what form non-radiative energy is transmitted by the chromosphere into the corona. The studies described above constrain wave energy fluxes, while imaging of chromosphere and photosphere combined with modeling will constrain the forcing of the field into braids and twists by flows. Continuity over many hours and a large thermal range of the spectroscopic diagnostics from chromosphere to corona are essential to follow the chromosphere's evolution.

IRIS will also shed light on how and where non-thermal energy is first released. Non-radiative energy deposited into the corona is lost both by radiation and by transfer into the lower layers of the solar atmosphere. The transport to the lower layers can be by thermal conduction, in which case we expect a relatively smooth temporal evolution (although spatial gradients may be large) leading to 'evaporation' of warming material from the top of the chromosphere. Alternatively, energy can propagate downward as energetic particles that can penetrate into the high chromosphere; these particle precipitations are likely more intermittent as they rapidly shift in position.

Some recent studies suggest that heating to coronal temperatures occurs primarily in the chromosphere proper[42]; one may expect this scenario to lead to explosive evaporation[37], or to thermal gradients that for some time will have extrema lying within the chromosphere.

Spectroscopic studies at high spatio-temporal cadence covering a large range in temperatures will help us differentiate between these scenarios, and thus shed light on heating processes throughout the solar atmosphere, even though the primary focus is on the chromosphere and low TR.

IRIS spectra will be directly compared to forward models of optically thin and thick spectral lines to understand the line-centroid Doppler shifts and the line shapes for a variety of solar conditions seen from different perspectives depending on the position on the Sun. This, combined with studies of the statistical properties of line-broadening as a function of temperature, viewing angle, underlying structure, and temporal evolution will allow us to determine the dominant cause(s) of non-thermal line broadening, whether it be unresolved flows, waves, turbulence, or other. The interpretation of the line shapes and shifts will greatly benefit from the high spatial, temporal, and spectral resolution offered by IRIS. The characteristic spatial resolutions of, e.g., SOHO/SUMER and Hinode/EIS are equivalent to ~18 IRIS resolution elements (x6 along the slit and x3 perpendicular to it). The high throughput enables IRIS to study wave phenomena up to ~250 mHz for a fixed slit position and up to ~50 mHz in its 4" dense raster mode (see Fig. FO2-1). Thus residual causes for non-thermal line broadening will be limited to superposition of structures less than about 250 km and/or wave periods far above the dominant 3 mHz oscillation spectrum.

The interpretation of such line broadenings will be guided by comparing a variety of environments and perspectives. For example, propagation effects can be studied both by comparing phases and relative amplitudes of changes in line broadening at the full range of IRIS temperatures; by a statistical comparison of observations towards the limb to those nearer to disk center to disentangle the relative roles of longitudinal and transverse broadening effects; by an analysis of line shapes and shifts with height above the limb and with formation temperature; and by the comparison of line shapes in different circumstances, including network-plage contrasts and differences between quiescent and flaring conditions. Similar recent studies at the lower resolutions of EIS[78, 79] and SUMER[31] demonstrate the potential: blueshifts and non-thermal broadenings in an active region decrease towards the limb, which supports the concept of evaporative upflows in response to intermittent heating, while a nearly isotropic component in the line broadening in the quiet network suggests a ubiquitous mixture of Alfvenic waves and longitudinal motions. IRIS will be able to address this at higher resolution in the space, time, and wavelength domains.

IRIS's high-cadence observations will also vastly improve our ability to determine how much wave power is available to heat and accelerate the plasma in open-field regions at the base of the solar wind: the measurements of transverse and longitudinal waves, and their possible couplings to the wind, will also provide constraints to models of the origin of turbulence in the heliosphere.

c) How do magnetic flux and matter rise through the lower atmosphere, and what role does flux emergence play in flares and mass ejections?

As magnetic field breaches the surface, it begins to interact and reconnect with the existing field into which it intrudes[43,34]. Observations suggest that reconnection begins shortly after flux emergence, i.e., when the field is barely protruding above the photosphere[44]. IRIS provides spectral coverage from the photosphere, throughout the chromosphere, into the low-temperature

corona. Thus, its spectroscopic raster maps can reveal the 3D flow patterns associated with flux emergence. The upflows in the low chromosphere of a few km/s[44,45,46], the associated downdrafts of the draining archfilament system at larger speeds[47], and the field expansion into the chromosphere and corona at Alfven speeds that exceed the sound speed of order 10 km/s[47,48,49], are all readily measurable within IRIS's design resolution of 0.5 km/s for chromospheric lines. These processes occur predominantly on Alfven time scales within the ~5000 km height range of the chromosphere; the IRIS imaging cadence of seconds and spectral rastering cadence of tens of seconds therefore allow us to follow these signals from the photosphere through the chromosphere.

These observations will also uncover the reconnection processes that happen early in the life of active regions (of which a sampling is likely to be observed during the mission life time, most frequently for new flux emerging into existing regions) down to small ephemeral regions (which are so frequent that many will be observed).

Emerging flux appears to play a key role in many flare phenomena[50-58]. Consequently, flare initiation also forms a natural target for an observatory that can see flux emerge from the moment that it breaches the photosphere to its penetration into the corona: chromospheric reconnection has been inferred in cases where emerging flux triggers a flare, and particle precipitation results in chromospheric ribbons both as tracers of coronal reconnections and as power sources for chromospheric evaporation. An observation of such flux emergence with Hinode revealed that the site of first energy release in a major flare occurred where strong electrical currents emerged[49]. IRIS's thermal range and high resolution will enable us to model how the atmosphere evolves in case of such a rapid energy release, and help constrain why flares are initiated where they are.

Flare forecasting has reached a state in which we can anticipate flares well enough to successfully point at many of them before they start[58]. This is demonstrated, for example, by the frequent TRACE observations of flares: TRACE views only 1/20th of the solar surface, but focusing on flare-prone active regions enabled it to capture over 60% of M and X class flares over the past 5y. SDO and Hinode vector-magnetograms will be available to the IRIS planners for this purpose.

As IRIS is designed to observe chromospheric emission, filaments and prominences are natural targets: their formation, dynamics, and eruptions can be studied with IRIS to deepen our understanding of the space weather that they drive, from associated flares to coronal mass ejections. IRIS can make spectral maps of filaments using its full slit length of 120 Mm to create large rastered maps at 1/3 arcsec steps in about 5 min., or can raster a smaller area to observe segments of filaments at higher time cadence. IRIS will be able to measure both line of sight and transverse displacements by combining spectroscopy and imaging, thus providing information on the three-dimensional structure of the filament's magnetic field, with potential differences between motions of ionized and neutral gases within the filament, where the plasma β is likely to bracket unity, resulting in a variety of flow-field couplings[59].

E.3 SCIENTIFIC REQUIREMENTS

To open new windows on the persistent problems areas in the coupling of photosphere and corona-heliosphere described above, IRIS must

- make significant advances in resolution in space, time, and wavelength;
- provide access to the entire chromosphere and the atmospheric regions around it, and
- embrace collaborations with complementing instruments and numerical modelers.

The primary science goals for IRIS are to connect the physics of photosphere and chromosphere to that of the TR and low corona. This requires simultaneous, co-spatial, sub-arcsecond images and spectra from the low chromosphere into the low corona. This dictates the use of the far-UV as one of the primary regions of interest: only there do we find an adequate sample of spectral lines within a narrow wavelength interval that span the bulk of chromospheric and TR temperatures from 10^4K to over 10^5K, with added select lines providing access to temperatures of about 1 MK and 10 MK [see top panel in Box III]. All of these emission lines stand out markedly above the surrounding continuum, and all are optically thin. These properties make comparison with numerical models straightforward.

The low-temperature chromosphere can be studied in any of its major cooling pathways, including Hα, Ca II H&K, Mg II h&k, and He 10830Å, but the instrumental and interpretational difficulties for these lines differ markedly. All but the Mg II lines are accessible from the ground, but ground-based observations of these other lines cannot meet the IRIS science requirements: it is not feasible to achieve and maintain alignment of space- and ground-based observatories to within fractions of an arcsecond along slits that span an

entire active region (120 arcsec for IRIS) for periods long enough to measure the evolution of the same features over their life time. Rastering over small areas would, ideally, yield some overlap of spectral maps of IRIS UV and GBO optical measurements, but then the sustained simultaneity that is needed to adequately track the rapid evolution and high-frequency wave propagation in the chromosphere would not be unachieved.

Apart from not offering the needed access to the higher temperature lines in the UV, the conditions required to achieve the needed resolution even for the lower-temperature chromosphere are only rarely met – and then only briefly - with a ground-based observatory; often weeks of observing yield only hours of high-quality data, and the best images are quite literally 'one in a million'. Another major problem is that although state-of-the-art adaptive optics, correlation trackers and post-observation reconstruction techniques (e.g., MOMFBD)[80] improve the quality of ground-based data dramatically, the images unavoidably suffer from sub-arcsecond artifacts and deformations associated with seeing that introduce ambiguities in the interpretation and still leave highly-variable and non-isotropic effective PSFs affecting the data. For example, hints of the sub-arcsecond displacements by Alfvenic waves in the chromosphere had been seen in ground-based data taken shortly before the launch of Hinode, but these remained unconvincing until Hinode/SOT provided data free from seeing artifacts[1]. Spectral information suffers from far more severe problems: image reconstruction techniques for slit spectra have not yet reached the required degree of sophistication.

The UV Mg II h&k lines, on the other hand, are well-suited for the IRIS science investigation. They are compatible with the IRIS science requirement of obtaining spectra and images of the low chromosphere. Their observation is achievable with continuous perfect alignment with the FUV observations within the SMEX budget at relatively little cost. The Mg II resonance doublet lines have superior qualities over the visible chromospheric diagnostics. The Mg^+ ion does not have a meta-stable upper state (as does Ca^+ associated with its infrared triplet) which simplifies its radiative transfer[81]; Mg^+ is not significantly affected by excitation through absorption of coronal emission (unlike He 10830Å; except during major flares); and the range of formation for Mg II h&k is much narrower than for Hα. In effect, the Mg II h&k lines are formed under effectively thin conditions (emitted photons escape, albeit subject to scattering) while having a ~20-fold higher opacity (mostly because of the higher abundance). Consequently, the Mg II h&k lines have a much higher contrast – relative to the Ca II H&K doublet – for small structures higher in the atmosphere, while being revealing such small structures over a larger range in optical depth because the lines are effectively thin[95,96]. In addition, we note that the broad wings of Mg II enable tracing of perturbations from the upper photosphere into the upper chromosphere[82].

The current capabilities for numerical modeling of chromospheric radiative transfer are advancing rapidly. Some codes already include multi-ray 3D radiative coupling[83], time-dependent ionization[84], and magnetohydrodynamic effects[85]. In the years prior to the launch of IRIS, our co-I's will continue the development of their codes. For example, a massively-parallel version of the Oslo-group code is already in a stage of advanced testing. The hundredfold improvement in wall-clock time of this code will allow 3D radiative-MHD simulations at much higher spatial resolution and scales, and for a wider variety of magnetic field configurations, than is currently possible.

The measurement requirements (see Table FO1-1, with sample observing sequences in Table FO2-2 and Fig. FO2-1) and the instrument and mission functional requirements (see also the mission traceability matrix in Table FO1-2) are:

1. Angular resolution and field of view. Hinode SOT and La Palma observations reveal structure down to their angular resolution of near 0.2″ and 0.16″, respectively. These highest resolution observations show that more than half of the observed chromospheric features have widths that exceed 0.3-0.4 arcsec[7], which is the resolution that we can achieve within the SMEX envelope. IRIS will obtain 0.33 arcsec resolution in the far-UV (Nyquist limit), and between 0.33 and 0.4 arcsec in the near-UV (diffraction limit) depending on whether structures are linear or point-like. At that resolution, IRIS will provide a major leap forward relative to existing spectroscopy instrumentation for the chromosphere and TR. Moreover, observations combined with numerical studies will help us evaluate sub-resolution structure.

The slit-jaw images and the slit length must extend over the length of a large active region, i.e., over up to 120 Mm. Oversampling of the resolution by a factor of two, yields a minimally required detector width of 1,000 pixels.

2. Temporal resolution, throughput, rastering. Hinode Ca II H observations show that a temporal resolution of better than 10s is required; at 20s cadence, many of the high-chromospheric fibrils can no longer be unambiguously traced in time.

Both Hinode and TRACE frequently observe chromospheric plasma with apparent velocities of 100-150 km/s in active regions. These may be real or apparent velocities of shifting brightness signals. To differentiate between these, and to follow their evolution with pixels of 0.16″, the maximum allowed active-region exposure time is ~1s.

Anticipated transverse oscillatory motions of up to an arcsecond, and a typical spacing of photospheric footpoints by a granular scale of one arcsecond, suggest that the spectrograph must raster an area of several times (say 3×) that length scale within the required 10s cadence for raster images. Sampling that area with 1/3 arcsec steps, requires raster steps at a cadence of ~1s.

3. Spectral resolution, wavelengths, stability, and calibration. IRIS must observe spectral lines from photosphere to low corona with particular focus on the chromosphere to low TR with little contamination from a continuum, within as compact a wavelength range as possible to minimize detector and telemetry requirements. These requirements are met for the ranges of 1332-1358 Å and 1380-1406 Å (see Table FO2-1).

In addition to these optically thin lines, we require access to one of the major radiative leaks from the chromosphere. The Mg II h/k resonance lines around 2800 Å are well suited for this, and compatible with an instrument designed for UV spectroscopy. Like the Ca II H/K lines, these lines are collisionally excited within the chromosphere, and their wide wing profiles contain contributions from the upper photosphere to the upper chromosphere. With an Mg abundance that is 14× that of Ca, and because the Mg II h&k lines have higher strengths than the Ca II H&K lines, the optical depths are at least an order of magnitude larger in Mg. This makes Mg II more sensitive to higher layers, which is a very attractive quality given the faintness of the high fibrils seen off limb in the Hinode Ca II H data. Lines in the wings of the Mg II doublet provide information on the upper photosphere, so that a 50Å wavelength window around the strong 2796Å line will provide an excellent complement to the far-UV window.

To access thermal line widths from the mid-chromosphere at *log(T)*~4 upward, a spectral resolution of ~40 mÅ is required in the far-UV and double that for the near-UV channel. For acoustic waves at 10^4, 10^5, and 10^6K, respectively, the corresponding wavelength shifts at sound speeds of 9, 30, and 90 km/s are 40, 140, and 430 mÅ at 1400 Å, and twice that around 2800 Å, compatible with the above resolution requirement.

The exchange of mass with the corona includes upflows from gentle evaporation to explosive flare responses as well as downflows in coronal rain and post-flare loops. IRIS needs to measure Doppler shift variations to a fraction of the sound speed, say to ~0.5 km/s, requiring stability to that level over the duration of hours (i.e., throughout an orbit). To observe these, ~800 photons should be detected within an exposure[60] (see Fig. CSR-B (page E-8) for simulation results). Relative wavelength calibrations can be made for every observing interval by observing neutral emission lines in the far-UV channel and neutral absorption lines in Mg II line wing spectra, provided that these observations average over periods much longer than granular evolution (and subject to corrections for the asymmetry of up- and downflow brightness[61,62,63] - this can be both modeled and corrected for by center-to-limb observations).

The absolute wavelength will be achieved by pointings at multiple limb positions as well as multiple near-photospheric neutral lines in the Mg II line wings, combined with occasional pointings at stellar sources (e.g., white dwarfs).

4. Slit-jaw bandpasses and resolution. Slit-jaw images at 1/3 arcsec resolution are needed in bandpasses around 1350 Å (C II and Si IV, both TR, with FWHM of 40 Å), the Mg II k line (2796 Å, chromosphere) and Mg II wing (2816 Å, photosphere). We take the brightness of the Ca II H spicules observed off limb by Hinode as a measure for faintest signatures we wish to observe on disk. If we use the ratio of that signal to the on-disk Ca II H images to estimate how strong they should be relative to the line-wing contributions to show up at 30-50% of the total signal on disk, and scale to Mg II k line properties, we find that the FWHM passband for Mg II k should be no wider than 15Å. In fact a 5Å passband is achieved with a Solc/Lyot plus prefilter in the Mg II k beam. This narrow passband results in much higher contrast of chromospheric to photospheric signal.

5. Effective area. The spectrograph effective area should enable acquiring ~800 photons (see point 3 above) per resolution element per 0.5s exposure for a set of strong lines. Table FO2-1 shows that this is achieved for active regions, our primary target class, with a design based on a 20-cm

IRIS observables: spectra, images, and sample observing sequences

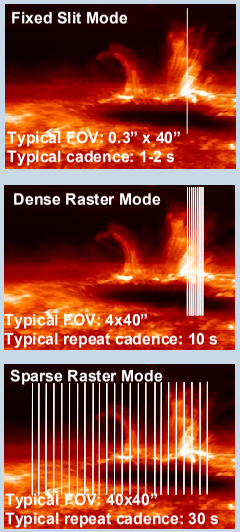

Ion Spectrum	λ Å	Δλ mÅ	Log T K	Estimated Count Rate (counts/s/line/spatial pixel) Quiet Sun	Active Region	Flare	Detector
UV Spectra (effective area of 2.8 cm² for far-UV, 0.3 cm² for Mg passband, continuum is 1 Å) †: Count rates for Mg II wing, h and k are in counts/s/spectral pixel/spatial pixel							
Si I (3P) Cont	1335	12.5	3.7	40	80	---	1
Mg II wing	2820	25	3.7-3.9	2100†	7500†	7500†	3
O I	1356	12.5	3.8	50	100	250	1
Mg II h	2803	25	4.0	870†	3400†	13000†	3
Mg II k	2796	25	4.0	1100†	4500†	10000†	3
C II	1335	12.5	4.3	540	1970	22000	1
C II	1336	12.5	4.3	500	1780	20000	1
Si IV	1403	12.5	4.8	400	1000	1e6	2
Si IV	1394	12.5	4.8	640	2200	3e6	2
O IV	1401	12.5	5.2	65	116	2e5	2
O IV	1400	12.5	5.2	25	60	1e5	2
Fe XII	1349	12.5	6.2	30	50	500	1
Fe XXI	1354	12.5	7.0	10	40	4e4	1
UV Slit-Jaw Images				**Estimated Count Rate (counts/s/pixel)**			
Effective area 0.005 cm² with 4 Å FWHM filter for Mg II; 0.7 cm² with 40 Å FWHM for far-UV.							
Mg II wing	2831		3.7-3.9	2300	5300	5300	4
Mg II k	2796		4.0	750	3500	8500	4
C II	1335		4.3	400	1300	13000	4
Si IV	1400		4.8	300	1200	2e5	4

Fig. FO2-1 IRIS spectrograph observing modes *depicted on a Hinode/SOT image. Step size and exposure times are flexible.*

Table FO2-1 Count rates for strong spectral lines (top) *are compatible with the required 1 s raster cadence (see §E.3). Count rates are based on atlas data assuming a filling factor of 1/3 (i.e., assuming thin linear structures). Count rates will scale with the actual filling factor on the Sun. The dominant lines Mg II k, C II, and Si IV contribute 50% or more to their respective slit-jaw images.*

Table FO2-2 Sample IRIS observing sequences and modes. *IRIS's design enables flexible sequences, moving the spectrograph slit to raster different fields of view at different step sizes, from 0.17" upward (Fig. FO2-1)*

Theme (FO1-1)	Science objective	Observing details Image size / cadence λ Range (FUV+NUV)/cadence	Spectrograph mode Raster stepsize / range Cadence / duration	Dataflow: Rate On-board memory margin Passes that can be missed
A	Measure energy of longi-tudinal & transverse waves	1335 Å &1400 Å: 384x512/ 20s Mg II k & wing: 384x512/ 20s Spectrograph: 4 Å+2 Å / 1s	*Dense Raster (rotation tracking)* 0.33" steps / 6.6"x85" 20 s raster cadence / continuous	*Baseline: 0.7 Mbit/s* 90% (if no passes missed) 1 pass/day for 10 days
A	Study microflare heating in chromosphere, TR and corona	1335 Å &1400 Å: 512x1024/10s Mg II k & wing: 512x1024/10s Spectrograph: 7 Å+4 Å / 1s	*Dense Raster (rotation tracking)* 0.33" steps / 5"x171" 15 s raster cadence / 5 hours	*Transient: 2.7 Mbit/s* 19% (if no passes missed) 2 of 2 passes for 5 hours
B	Study the formation and impact on transition region of spicules, surges and upflows	1335 Å &1400 Å: 256x512/15s Mg II k & wing: 256x512/15s Spectrograph: 4 Å+2.5 Å / 1s	*Dense Raster (rotation tracking)* 0.33" steps / 4"x85" 12 s raster cadence / 10 hours	*Minimum: 0.7 Mbit/s* 90% (if no passes missed) 5 of 5 passes for 10 hours
C	Study the evolution of promi-nences: motion in legs, re-connection signatures, waves	1335 Å &1400 Å: 384x512/20s Mg II k & wing: 384x512/20s Spectrograph: 8 Å+4 Å / 2s	*Sparse Raster (rotation tracking)* 1" steps / 18"x85" 36 s raster cadence / 1 week	*Modified Baseline: 0.7 Mbit/s* 90% (if no passes missed) 1 pass per day
C	Study flux emergence and flare/CME response	1335 Å: 512x512 / 2.5s Mg II k & wing: 512x512/10s Spectrograph: 8 Å+5 Å / 1s	*Sparse Raster (rotation tracking)* 2" steps / 24"x85" 12 s raster cadence / 12 hours	*Modified Transient: 1.5 Mbit/s* 19% (if no passes missed) 3 of 6 passes for 12 hours

P80133_050_FO_3

IRIS science investigation: expertise and coordination

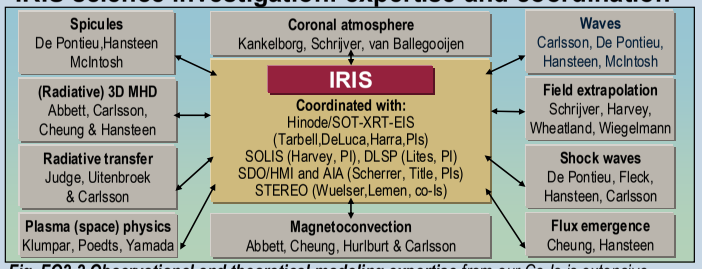

Fig. FO2-2 Observational and theoretical modeling expertise *from our Co-Is is extensive and will support the interpretation of IRIS data complemented by other missions.*

Table FO2-3 The IRIS Investigation Science Team.

Team member	Affiliation	Responsibilities/Expertise
Title, A	LMSAL	**Principal Investigator**
Cheung, M	LMSAL	Numerical modeling flux emergence
De Pontieu, B	LMSAL	Analysis of data/models
Freeland, S	LMSAL	Analysis software system (SolarSoft IDL)
Hurlburt, N	LMSAL	Data archiving
Lemen, J	LMSAL	Instrument scientist
Schrijver, C	LMSAL	Science lead
Shine, R	LMSAL	Operations lead
Tarbell, T	LMSAL	Inter-experiment coord.; PI Hinode-FPP
Wuelser, J-P	LMSAL	Optics design
Tenerelli, D	LMMS	Spacecraft design, construction, integration
Kankelborg, C	Montana State University	Spectrograph
Klumpar, D	Montana State University	Student Collaboration lead; Plasma physics
Abbett, W	University of California, Berkeley	Numerical modeling (radiative MHD)
Harvey, J	National Solar Observatory	Chromospheric field obs.; PI SOLIS
Uitenbroek, H	National Solar Observatory	Chromospheric radiative transfer models
Lites, B	High Altitude Observatory	Coordinated vector magnetography
Judge, P	High Altitude Observatory	Spectroscopic analysis and modeling
McIntosh, S	High Altitude Observatory	Wave analysis
Scherrer, P	Stanford University	SDO/HMI coordination; PI HMI
Golub, L	Harvard SAO	Main telescope design
DeLuca, E	Harvard SAO	Hinode/XRT coordination; PI XRT
Weber, M	Harvard SAO	Data analysis
van Ballegooijen	Harvard SAO	Field & filament modeling
Yamada, M	Princeton University	Plasma physicist; reconnection physics
Tsuneta, S	National Astron. Obs. Japan	Hinode/SOT coordination; PI Hinode
Carlsson, M	Inst. Theoretical Astrophys., Oslo	MHD and radiative transfer modeling
Hansteen, V	Inst. Theoretical Astrophys., Oslo	MHD modeling; ground-station coord.
Fleck, B	ESA, Space Science	ILWS/ESA coordination
Harra, L	Mullard Space Science Laboratory	Hinode/EIS coordination; PI EIS
Wiegelmann, T	Max Planck Inst. Solar Syst. Res.	Vector-field modeling
Wheatland, M	University of Sydney	Vector-field modeling
Poedts, S	Centre Plasma Astrophys., Leuven	Plasma physics; MHD/multi-fluid modeling
Waltham, N	Rutherford Appleton Laboratory	Camera design; consulting
Worden, S	NASA Ames	Mission Operations

aperture telescope; for quiet-Sun observations exposures of 1-2s or on-chip summing can be used.

6. Continuity, coverage, and telemetry. Continuous high-cadence observing should be sustainable for at least 8 hours per day. For a characteristic observing sequence of 2 slit-jaw images of 512×512 pixels compressed to 3 b/pix per 10s plus one spectral frame per second of 1024×512 pixels (for a selection of 8 strong lines) compressed to 3 b/pix, telemetry would accumulate at 1.65 Mb/s. We note that 3b/pix compression results in very high-quality data; for comparison, the Hinode SOT-SP spectro-polarimetric data, with much higher S/N requirements than needed for IRIS, is typically compressed to 2.3-2.7 b/pix. A run of 8h (enough to cover a substantial flux emergence, a typical flare, or more than a thermal time scale for long coronal loops) would require ~46 Gbit in total. To downlink this using passes of typically 8 min each at 10 Mb/s would require ~16h. Examples of other observing sequences (Table FO2-2) show that the science goals can be met by telemetry rates near 70 Gb/day using 13 downlink passes per day, with transient campaign modes of up to 5h duration requiring an onboard memory of 48 Gb. IRIS' nominal data rate far exceeds that of current spectrographs (Fig. FO1-4).

The near-terminator orbit of IRIS will lead it through the high-radiation environment of the high-latitude auroral zones on every orbit and of the SAA on many of its orbits. A decade of experience with TRACE in a very similar orbit has demonstrated that the timing of these radiation zones is accurately predicted, so that the instrument can be paused during these times, if desired. However, IRIS' baffling and shielding is much better than those of TRACE, and the typical exposure times a factor of ten or more shorter than for TRACE, so that the radiation effects will be much less severe, and in many cases IRIS may be operated through the high-radiation zones. Also, the on-board software can respond to times of high radiation: special-purpose readouts of unexposed parts of one of the CCDs can determine the radiation level, and science observing can be paused until such exposures show the radiation level to have dropped to acceptable levels.

As IRIS can be paused during high-radiation times, spectral raster maps can be obtained without spatial gaps. The temporal gaps will cause irregularity of the cadence of the observations, but since oscillations within the chromosphere and TR are typically not coherent beyond 1 hour, the impact of this on the scientific analysis will be limited.

7. Spacecraft requirements. Spacecraft rolls of up to 90º may be required approximately once per week to rotate the spectrograph slit relative to the target. This enables aligning the slit with the near-vertical structures at the east or west limbs, and with loop systems in emerging active regions. Other roll angles would be required at the polar limbs or when rastering, for example, filaments.

8. Mission duration. We propose a baseline mission of two years to obtain an adequate sampling of flux emergences, flares, filaments and their eruptions, and coronal holes. A second year of operations allows the team to optimize observing sequences in response to community suggestions based on the publication of first results.

9. Coordinated observations. IRIS data contain a wealth of information by themselves. However, combination with other observables will clearly increase the discovery space for IRIS and for the coordinating missions. Key complementary observables are photospheric and chromospheric magnetograms. IRIS is expected to overlap with the SDO/HMI vector-magnetograph with 1 arcsec resolution, and will benefit from ground-based chromospheric line-of-sight magnetograms with, e.g., SOLIS. There is also a major benefit to coordinating with Hinode-SOT which can obtain filter- and spectrograph-based vector-magnetograms at 0.2 arcsec resolution. If Hinode is operational when IRIS flies, a joint operations system will be implemented to optimize coordinated observing.

IRIS has access to Fe XII and XXI lines to observe the chromosphere-corona coupling. SDO's AIA will provide context information with comprehensive thermal coverage in its 6 Fe-line passbands. Spectral information for the corona will be obtained by coordinating with Hinode's EIS.

Apart from operational requirements, coordination needs also have implications for the launch opportunity: A mission from 2012 to 2014 means that Hinode will be 5-7 y old, SDO 3-5 y, with the solar cycle likely around maximum. A later launch will reduce the number of large flux-emergence and explosive events that can be targeted as the solar cycle proceeds to its declining phase, and it will increase the risk that Hinode or SDO will fail or be terminated. If the context data for photospheric vector field or coronal responses would have to be obtained with lower-quality ground-based and space-based alternatives (such as SOLIS, ATST, or the GOES coronal imagers), this would negatively impact our investigation.

Table E-1 Downscopes (ranked by priority) leading to a Minimum Science Mission (see Sec. E.5).

Option	Impact	Phase	Estimated savings Cost M$	Mass kg
Common camera	Reduced flexibility in scientific operations; fixed synchronicity	A	0.99	7.8
Reduced telemetry	Reduced number and variety of events	E	2.6	-
1 imaging channel	Loss of travel-time studies in surroundings; reduced context.	A	0.55	7.5
Shortened mission	Reduction in number and variety of events	E	3.9	-

The IRIS co-I team is committed to optimal coordination with other observatories to obtain (vector-)magnetograms. For SDO such coordination is straightforward: SDO/HMI observes the full Sun continuously, making line-of-sight magnetograms every minute and vectormagnetograms every 15 min. in its standard operating mode, with cadences fast enough to measure (super-)granular flows and flux emergence. The IRIS data will share the storage facility and access interfaces with the SDO/HMI and AIA projects; and the PI and several co-I's of HMI are part of the IRIS team. Coordination with Hinode's SOT/SP and NFI is facilitated similarly: the SOT data archive is at LMSAL, the SOT PI and SP PI are members of the IRIS team, and operational planners for Hinode are part of, or in close contact with, the LMSAL team. For coordination with, e.g., SOLIS and the future ATST, we benefit from NSO co-I's Harvey and Uitenbroek. We plan on regular weekly teleconferences, with monthly longer-term planning components, to ensure the necessary coordination between these various observatories.

10. Numerical and laboratory experiments. The IRIS investigation includes an extensive numerical radiative MHD and plasma-physics component to enable full-forward modeling of the domain from the top of the convective envelope to the low corona. To ensure a solid foundation for this modeling, and to validate the findings in combination with IRIS data, we include multiple world-class modeling efforts within the co-I team (Fig. FO2-2, Table FO2-3, §D.6.3). The funding of this modeling complement during mission development and operation is as important as meeting the above instrument requirements. The IRIS investigation also embraces laboratory plasma physics expertise to guide data interpretation by benefiting from the expert knowledge of that community. We foresee the routine computation of high-fidelity field extrapolations by non-linear force-free methods and magnetostatic models[64,49,65] as an important ingredient to provide constraints on the photosphere to corona pathways of the field.

Because the main goal of IRIS is understanding the physics of the chromospheric region around β=1, our efforts will naturally involve the development of advanced models to deal with forces acting on the field within this region.

The substantial numerical component of the IRIS investigation will be managed through a series of dedicated working-group meetings, each progressing based on findings from preceding meetings, with the goal of advancing, testing, and implementing the increasingly mature numerical codes for the use of data interpretation. The completion of these codes in time for the data analysis effort will be viewed as 'deliverables' by the PI team and developers, with an initial schedule outlined below. The management of this aspect will build on the very successful concept used for the advancement of nonlinear force-free field modeling (NLFFF): experts from around the world are brought together for a regular series of small workshops with a dozen participants, to model carefully designed test cases, interpret the model results, publish the findings, and design a more advanced test case for a subsequent meeting. While continuing the NLFFF series for Hinode and SDO as well as for IRIS, we plan to also bring together the modeling subgroups on interior-to-corona radiative MHD, on radiative-transport, and on models for, e.g., chromospheric dynamics and filaments. Models will also be compared with available observations from GBOs, Hinode, and - soon - SDO. The modeling teams will be involved in discussion that determine data products, and their model runs will provide input to test algorithms to interpret line shapes and Doppler shifts, and to test the performance and biases of analysis algorithms.

The rapid advances in computational infrastructure and algorithms have revolutionized the state-of-the-art of numerical simulations and the role these play in interpreting and explaining observations. These advances are dramatically reducing the idealizations and simplifications that are made in order to enable the computations. Present-day simulations include (sub-)photospheric

convection and have open boundary conditions [Abbett and Oslo], while approximating non-LTE radiative transfer[85, 86]. These state-of-the-art models already tackle major problems such as flux emergence[43, 46], physics of the outer atmosphere[7, 43] including the corona[87], the low-chromospheric wave heating[24, 88], the morphology and dynamics of chromosphere and transition region, including jets[7, 10, 84, 89].

Members of the IRIS team are at the forefront of the most advanced numerical codes that are available for the solar atmosphere (Oslo-group, and Abbett). The Oslo code is supported by 3 tenured professors (funded by Oslo University) and 2 post-docs (from Norwegian and European funding sources). Over the past 5 years, the efforts of the Oslo team have been closely aligned with the observational expertise at LMSAL[1, 2, 7, 10, 24, 89, 90, 91, 92,, 93]. This collaboration includes frequent mutual visits of up to a few months in duration, as well as a joint project at NASA's Columbia supercomputer. We plan to intensify this collaboration with IRIS.

Recent progress in parallelization (MPI) and the availability of massively parallel supercomputers will enable major advances in spatial resolution, the study of a wide range of magnetic field configurations, and an increased volume of the simulation domains. Advanced versions of both the Oslo-group and Abbett codes are being worked on, with MPI versions functional by 2009.

To further increase the realism of the numerical simulations, the IRIS project will expand the Oslo code to include a neutral component starting in 2009. This multi-fluid approach will enable the detailed treatment of a generalized Ohm's law that includes the Hall and Pedersen conductivity, both of which increase the resisitivity in the partially-ionized chromosphere[94]. This is expected to be complete by 2011.

In parallel, IRIS will support advancing the realism of the Abbett code, which takes a more parametrized, but computationally faster approach to the physics of the interface region. This model allows for larger statistical studies of the impact of magnetic field configurations on the transition region and corona. This parallel approach broadens the range of models to support the interpretation of IRIS data.

The advanced state-of-the-art, the complementary computational approaches, the clear path towards more realistic simulations of the interface region, the anticipated increase in computational power by Moore's law, and the efforts devoted by the experienced IRIS co-I's to the development of these simulations, will lead to the implementation of an efficient, high-fidelity numerical laboratory in support of IRIS even before its launch.

E.4 SCIENTIFIC DATA AND OTHER SCIENCE PRODUCTS

The scientific data of IRIS consist of spectra and slit-jaw images. These form the basis of the science investigation after zero-point corrections and calibration procedures are applied. The data will be relayed from the Svalbard ground station to the SDO Joint Science Operations Center at Stanford as raw telemetry files. They will then be processed into spectra and images, and calibrated to level 1 as part of a JSOC data pipeline for IRIS. Level 1 IRIS data in standard FITS format will be freely available to the research community via the Internet within 24 hours of receipt by the JSOC. These data will be directly readable and useable through standard SolarSoft IDL routines.

Descriptions of the observations including critical planning information, data quality and quick-look assessment will be provided using systems derived from the Hinode Observation System, while event and feature meta-data will be part of the heliophysics knowledge base being developed for SDO (§E.6.3). Calibration and other related instrument details will be published on the web following guidelines for the Hinode mission.

E.5 MINIMUM SCIENCE MISSION

A minimum valuable investigation is reached upon these down scopes, listed in order of increasing impact on the science return (see Table E-1):

a) Instrument: Single camera. The spectral and slit-jaw detectors can, in principle, be read from a single camera. This imposes a fixed synchronicity on image cadence (but does not impact the ability to expose each detector as needed because they have dedicated shutter systems). Savings in cost and mass can be achieved with this option if implemented early in the design stage.

b) Ground system: Cost saving on telemetry. A reduction in the number of down-link passes will lower cost during phase E; a minimum of 8h observing per day at nominal data rate must remain possible, requiring at least 5 passes per day. An alternative cost-saving that we will pursue first is the possibility to (partially) fund the down-link station at Svalbard through collaboration with the Norwegian Space Agency and ESA; if this option is successful, the achieved savings will be used to augment data analysis and modeling.

c) Instrument: Single-channel slit-jaw camera. Omission of the filter wheel in front of the slit-jaw

camera lowers cost and mass if considered early in the design phase. In principle, having either the Mg II k 2796 Å or one of the far-UV band passes suffices for detailed co-alignment with observations made by other observatories. Which diagnostic would have the smallest impact on the science plan will be determined by the investigator team should this option be considered.

d) Mission: Reduction to 1-year mission. Shortening the baseline mission duration to 1 year reduces the number and variety of events observed proportionally. As data analysis and modeling efforts require 2 years, the cost savings in this case lie primarily in mission operations.

Implementation of these options results in a mission in which (option **a**) the reduced flexibility of spectral rastering and imaging lowers raster repeat frequencies and/or image cadence so that rapid, impulsive phenomena are less well observed, (option **c**) differential timing studies (travel-time studies, flare-ribbon propagation at different temperatures, or post-reconnection evolution) for areas around the slit-jaw position are no longer possible, while (options **b** and **d**) the number and variety of events observed are reduced in proportion to the telemetry. Options not listed are considered not viable for a minimum science mission (e.g., a non-polar orbit would not offer the required continuity of observations; no lower-cost launch vehicle is available).

Note, no changes are made to the next section, §E.6, except for updates to Fig. FO3 (foldout). ***If anything in §E.6 conflicts with §F regarding technical details of the implementation, §F takes precedence.***